Materials Science & Engineering A 674 (2016) 144–150

Contents lists available at ScienceDirect

Materials Science & Engineering A

journal homepage: www.elsevier.com/locate/msea

Deformation behavior and characteristics of sintered porous 2024 aluminum alloy compressed in a semisolid state

Min Wu [a,b], Yunzhong Liu [a,*], Teng Wang [a], Kaibin Yu [a]

[a] National Engineering Research Center of Near-net-shape Forming for Metallic Materials, South China University of Technology, Guangzhou 510640, People's Republic of China

[b] College of Materials and Chemical Engineering, China Three Gorges University, Yichang 443002, People's Republic of China

ARTICLE INFO

Article history:
Received 27 May 2016
Received in revised form
15 July 2016
Accepted 28 July 2016
Available online 29 July 2016

Keywords:
Semisolid compression
Sintered porous material
2024 aluminum alloy
True stress–strain curve
Constitutive equation

ABSTRACT

Semisolid powder forming technology is a novel technology that has achieved a great progress in recent years. However, the deformation behavior and constitutive model governing semisolid powder forming remain unclear. Sintered porous 2024 aluminum alloy specimens with different initial relative densities were compressed at 580–600 °C in a semisolid state at strain rates of 0.1, 1, and 5 s^{-1}. The results indicate that the solid skeleton of the sintered porous material deforms elastic-plastically in stage I ($\varepsilon < \varepsilon_{c1}$) without breakup of the solid skeleton and powders. In stage II ($\varepsilon_{c2} > \varepsilon > \varepsilon_{c1}$), the solid skeleton is broken up and the powders rupture. Then, the liquid is squeezed out, and it flows and fills the gaps/pores, resulting in higher relative density. In stage III ($\varepsilon > \varepsilon_{c2}$), powders are crushed into fragments and the liquid flows from the edge to the surface of the samples. Then, new pores appear, decreasing the density of the samples. The constitutive equation is modified by introducing variables of liquid fraction and relative density, and it agrees well with the measured data.

1. Introduction

As a promising technology, semisolid powder forming has the advantages of powder metallurgy and semisolid formation, such as fine grains, net-shaping, and short process. At present, most investigations in this new area are concentrated on the process, microstructure, and mechanical properties. However, theoretical investigations on the semisolid powder forming process are very few. Hamilton et al. [1,2] simulated the semisolid powder forming process by considering semisolid powders as the Newtonian liquid, which is more suitable for higher liquid fraction (> 60%). Wu and Kim [3] investigated the compaction behavior during semisolid closed die compaction with the Shima–Oyane model, which describes the relationship between compaction pressure and relative density. Luo and Liu [4,5] studied the densification process and mechanisms during semisolid powder rolling, and achieved the relationship between deformation strain and relative density. However, their models relate only to densification, while the deformation constitutive model considering stress, temperature, strain rate, and relative density is not available.

The uniaxial compression test is a basic experimental method to analyze theoretically the deformation behavior of a complicated formation process. Thus, many investigations were carried out to study the deformation process, mechanism, and constitutive model of aluminum alloy bulk materials compressed in a semisolid state [6–12]. However, very few studies have concentrated on semisolid compression of porous materials or powders. Their deformation behavior and constitutive model are different from those of bulk materials because of the existence of pores and the difference in liquid distribution.

To investigate the deformation behavior of semisolid powder forming and to simulate the forming process, isothermally uniaxial compression of sintered porous 2024 aluminum alloy was conducted at semisolid temperatures in this study. The sintered porous materials were prepared from gas-atomized powders by spark plasma sintering (SPS). The true stress–strain curve of uniaxial semisolid compression and the microstructure of quenched samples were analyzed. On the basis of the above analyses, the deformation behavior of sintered porous materials under semisolid compression was discussed. The effect of initial relative density, strain rate, and deformation temperature on the true stress–strain curve was investigated. The constitutive equation was proposed and modified.

2. Experimental

The powders used are gas-atomized 2024 aluminum alloy powders with a near-spherical morphology (mean particle size

* Corresponding author.
E-mail address: yzhliu@scut.edu.cn (Y. Liu).

http://dx.doi.org/10.1016/j.msea.2016.07.120
0921-5093/

Table 1
Chemical composition of 2024 aluminum powders (mass fraction %).

Cu	Mg	Mn	Fe	Si	Zn	Ti	Cr	Al
4.09	1.18	0.54	0.21	0.12	0.06	0.02	0.10	Bal

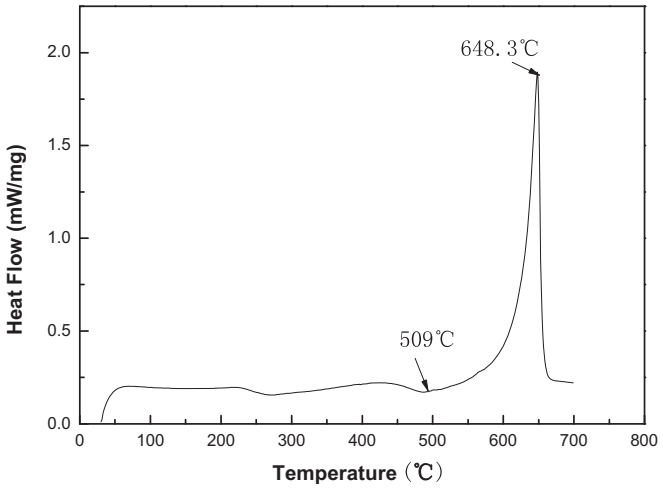

Fig. 1. DSC curve of 2024 aluminum alloy powders.

~75 μm). The chemical composition of the raw material is summarized in Table 1.

To measure the liquid volume fraction, the 2024 aluminum alloy powders were heated from room temperature to 700 °C at a rate of 10 °C/min by using STA 449C DSC equipment under argon gas flow at 20 ml/min to obtain the DSC curve (Fig. 1). This curve indicates that the actual freezing range of 2024 aluminum alloy powders is 509–648.3 °C, which is the basis for selecting the deformation temperature.

The 2024 aluminum alloy powders were sintered by Dr. Sinter Model SPS-825 SPS system (Sumitomo Coal Mining Co. Ltd., Japan) at 300, 400, and 440 °C for 2 min under vacuum (residual cell pressure < 8 Pa). The powders were heated at different heating rates (below 400 °C at the heating rate of 50 °C/min, above 400 °C at the heating rate of 20 °C/min). The microstructure of sintered powders is similar to that of the original powders, which is composed of fine equiaxed grains and shows a near-spherical morphology. The cylindrical compression testing samples with dimensions of 8×12 mm ($\Phi \times H$) were machined from sintered specimens. The relative density of each compression sample was tested using Archimedes' principle.

The semisolid compression tests were conducted using a Gleeble-3500 thermal simulation testing machine equipped with an electrical furnace. The cylindrical testing samples with aluminum-clad films were compressed at 580 °C, 590 °C, and 600 °C in a semisolid state at strain rates of 0.1, 1, and 5 s^{-1}, respectively. In each test, the samples were first heated to 500 °C at a heating rate of 200 °C/min, then to the objective temperature at a heating rate of 30 °C/min, and held for 3 min under the isothermal condition for heat balance before compression testing. Subsequently, the samples were quenched with water to retain the characteristics of semisolid deformed microstructure. The microstructure of samples etched by Keller's reagent was observed with an optical microscope (LcicaDM1500M). Scanning electron microscopy (SEM) test was performed using NovaNanoSEM430 to observe the fracture surface of the samples compressed in a semisolid state.

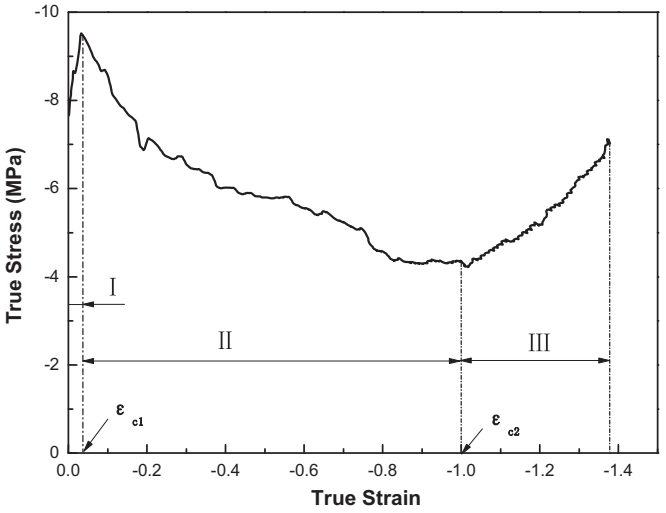

Fig. 2. True stress–strain curve of sintered porous 2024 aluminum alloy with initial relative density 68%, compressed at 580 °C with the strain rate of 1 s^{-1}.

3. Results and discussion

3.1. Deformation behavior during semisolid compression

Fig. 2 shows the true stress–strain curve of sintered porous 2024 aluminum alloy with the initial relative density of 68%, which was uniaxially compressed at 580 °C with a strain rate of 1 s^{-1}. It can be seen that the curve is not smooth, which might be due to the low deformation resistance and liquid flowing into pores/gaps. Similar phenomena were also reported by Tzimas and Zavaliagos [8] and Omar et al. [13]. The curve can be divided into three stages: in stage I, the stress increases rapidly with the increase in strain, until it reaches a peak value α_p (corresponding to the first critical true strain $\varepsilon_{c1}=0.032$); in stage II, when the true strain increases from 0.032 to 1.0 (the second critical true strain ε_{c2}), the stress decreases slowly; and in stage III, the stress increases again with the increase in strain. The liquid volume fraction of the samples at 580 °C is 10.5% (Fig. 3, which is calculated by an area integral of the DSC curve (Fig. 1)).

During stage I, the first critical true strain obtained from all the experiments falls in the range of 0.01–0.07, which is approximate to the bulk material (0.02 for SIMA AA2014 [11]). Tzimas and Zavaliagos [8] considered that the true strain at the peak stress is

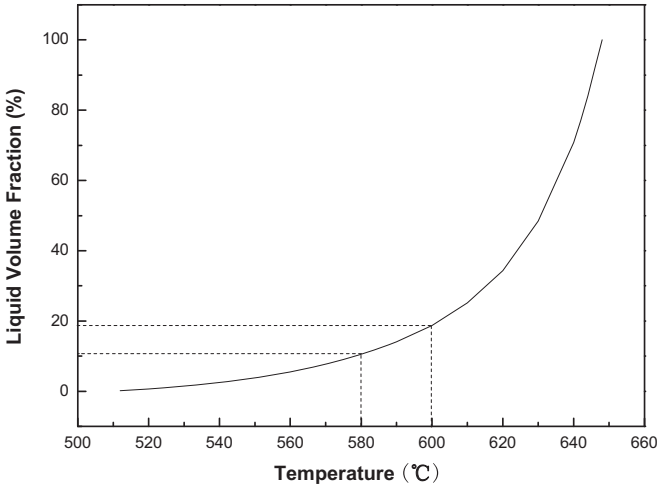

Fig. 3. Liquid volume fraction of gas-atomized 2024 aluminum alloy powders at different temperatures by DSC.